American Mineralogist, Volume 83, pages 365–372, 1998

Stacking disorder and polytypism in enargite and luzonite

MIHÁLY PÓSFAI[1,*] AND MARGARETA SUNDBERG[2]

[1]Department of Earth and Environmental Sciences, University of Veszprém, P.O. Box 158, H-8201 Veszprém, Hungary
[2]Department of Inorganic Chemistry, Arrhenius Laboratory, Stockholm University, S-106 91 Stockholm, Sweden

ABSTRACT

Microstructures of enargite and luzonite (Cu_3AsS_4) were studied using high-resolution transmission electron microscopy (HRTEM) and selected-area electron diffraction (SAED). Enargite and luzonite are intergrown at the atomic level in samples from Recsk, Hungary. Both minerals typically contain faults along the planes of their close-packed layers. Comparisons of electron micrographs and images simulated for several types of fault models indicate that the planar defects can be interpreted as stacking faults in the regular cubic (luzonite) or hexagonal (enargite) sequence of close-packed layers. In addition to disordered layer sequences, two long-period, rhombohedral polytypes—9R, $(21)_3$ and 24R, $(311111)_3$—occur in enargite. The presence of defect-free luzonite and enargite indicates that both minerals grew directly from the hydrothermal solution. The disordered structures represent transitional structural states between luzonite and enargite and probably reflect the effects of fluctuating conditions during hydrothermal deposition.

INTRODUCTION

Enargite and luzonite are polytypes of Cu_3AsS_4; they occur intergrown in many ore deposits. We wished to determine the microstructural and chemical characteristics of their intergrowths, because a better knowledge of these polytypic sulfides is useful for the understanding of conditions and processes that control ore formation in a hydrothermal environment. The structure-types of enargite and luzonite are widespread in nature and important in materials science. Luzonite crystallizes in a sphalerite-type, cubic close-packed (ccp) structure, whereas enargite has a wurtzite-type, hexagonal close-packed (hcp) structure. Luzonite is tetragonal (space group $I\bar{4}2m$, a = 0.533, c = 1.057 nm; Marumo and Nowacki 1967) and enargite is orthorhombic (space group $Pmn2_1$, a = 0.7401, b = 0.6436, c = 0.6154 nm; Adiwidjaja and Löhn 1970).

The similarities and differences between the two structures are best seen from a direction parallel to the close-packed layers (Fig. 1). The metal atoms are tetrahedrally coordinated by S in both structures; in Figure 1 the S tetrahedra project as isosceles triangles. Because the apices of all metal-filled tetrahedra point along the same direction, the two structures are non-centrosymmetric. Cu and As atoms occupy the metal positions in an ordered fashion. Half of the metal-atom columns that are parallel to $<110>_{luz}$ or $<100>_{en}$ contain only Cu atoms (marked X), and in half of them As and Cu atoms alternate (marked Y). The stacking sequences of S and metal layers that are parallel to $(112)_{luz}$ and $(001)_{en}$ can be conveniently described using the ABC notation for close-packed structures. If capital letters denote the positions of S atoms and lowercase letters represent metal atoms (in enargite and luzonite, As is considered a metal), the stacking sequence of luzonite is AbBcCaAbBcCa . . . , and the stacking in enargite is AbBaAbBa . . . .

Sb can substitute for As in the enargite structure by up to about 20 mol% Cu_3SbS_4 (Springer 1969); whereas a complete solid solution series exists between the ccp luzonite (Cu_3AsS_4) and famatinite (Cu_3SbS_4) (Gaines 1957; Lévy 1967; Kanazawa 1984).

Polysynthetic twinning is common in luzonite (Gaines 1957; Lévy 1967; Sugaki et al. 1982), and some enargite crystals show characteristic striations under the optical microscope (Sztrókay 1944). Our preliminary TEM studies (Pósfai 1991) indicated that samples from several localities (including Recsk, Hungary; Quiruvilca, Peru; Cosihuiriachic, Mexico) contain disordered luzonite and disordered enargite crystals.

The goal of the present paper is to study the nature of structural disorder by identifying the atomic structure of defects. A characterization of relationships between microstructures and compositions is given in another paper (Pósfai and Buseck 1998).

EXPERIMENTAL METHODS

We studied samples from the Lahóca Hill mine at Recsk, Mátra Mountains, Hungary. This locality is sometimes referred to as Mátrabánya (Springer 1969) or Parád (Lévy 1967) in the mineralogical literature. Enargite and luzonite occur together in the metasomatized ore bodies; enargite is dark brown or black and forms elongated, prismatic crystals. Luzonite occurs in pinkish gray masses. Macroscopic and optical characteristics of the two min-

* Current address: Department of Geology, Arizona State University, Tempe, AZ 85287-1404, U.S.A.

0003–004X/98/0304–0365$05.00

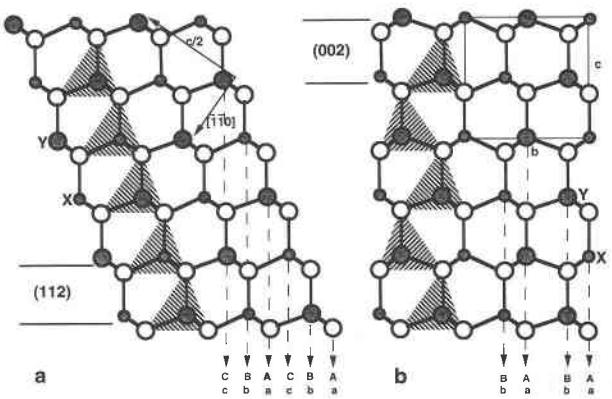

FIGURE 1. The structures of (**a**) luzonite and (**b**) enargite as projected along $[1\bar{1}0]_{luz}$ and $[100]_{en}$. Open circles = S atoms; filled circles = metal atoms. X and Y mark two types of metal-atom columns along the direction of projection; in X columns (small circles) there are only Cu atoms, whereas in Y columns (big circles) Cu and As atoms alternate.

erals are given by Sztrókay (1944). The Recsk porphyry copper ore deposit is described by Morvai (1982).

Mineral fragments were crushed and mounted on a copper grid covered by a holey-carbon film. Enargite specimens were prepared mostly from single crystals, whereas each luzonite specimen contained fragments of many crystals. Electron micrographs were obtained at 200 kV with a JEOL 200CX transmission electron microscope that has a top-entry, double-tilt specimen stage (±10°), a spherical aberration constant of 1.2 mm, and a structure resolution limit of 2.4 Å. The objective aperture used for high-resolution imaging has a radius of 0.41 $Å^{-1}$ in reciprocal space. Crystals were aligned to be viewed along the <110> or <201> directions of luzonite and <100> or <120> of enargite. The stacking sequences of close-packed layers can be directly observed in HRTEM images obtained from these directions. We simulated electron micrographs using a modified version of the SHRLI program (O'Keefe et al. 1978).

RESULTS

Fault models and image simulations

SAED patterns show diffuse scattering along [001]* of enargite and [112]* of luzonite (Fig. 2). The diffuse streaks indicate one-dimensional disorder; the defects occur along the close-packed layers, which are parallel to $(001)_{en}$ and $(112)_{luz}$.

Defects along the close-packed layers in related structures are commonly interpreted as stacking faults; examples include ZnS (Fleet 1977; Akizuki 1981; Qin et al. 1986; Pósfai et al. 1988), ZnSe (Mizera et al. 1984), and $CuInSe_2$ (Kiely et al. 1991). However, Aminoff and Broomé (1931) predicted that other types of planar faults, such as reflection twin boundaries could also occur in sphalerite- and wurtzite-type structures. Experimental evidence for the occurrence of reflection twins was first found in hcp BeO by Austerman and Gehman (1966).

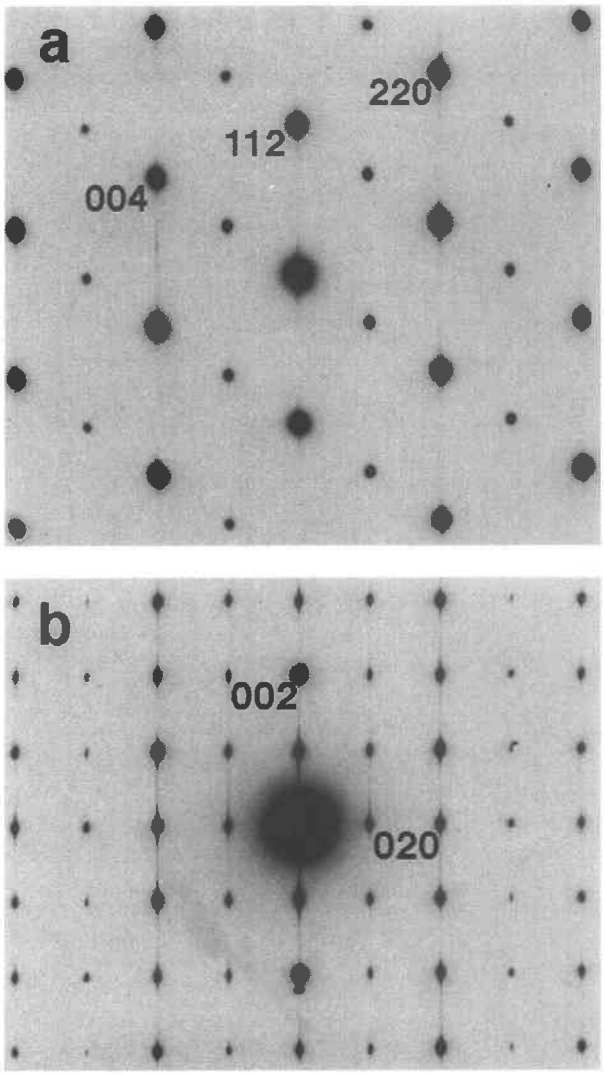

FIGURE 2. SAED patterns of (**a**) luzonite and (**b**) enargite obtained from $[1\bar{1}0]_{luz}$ and $[100]_{en}$. The diffuse streaks along $[112]^*_{luz}$ and $[001]^*_{en}$ indicate disorder in both structures. Streaks along $0kl$ with k = 3n are less pronounced than in other reciprocal lattice rows of enargite.

Shiojiri et al. (1982) presented HRTEM images of defects in ccp ZnSe that could be interpreted on the basis of a reflection twin-like structure model.

To be able to distinguish between different fault types, we carried out image simulations for ordered and faulted structures before obtaining HRTEM images. It is known from a vast body of literature on HRTEM imaging of sphalerite- and wurtzite-type semiconductors (Glaisher et al. 1989a, 1989b, 1989c; Smith et al. 1989) that in projections such as those in Figure 1, the image contrast is relatively simple in form and recurs periodically with changes in the values of objective lens defocus and crystal thickness. Through-focus series of simulated images are shown for ordered luzonite and enargite in Figure 3. The first pattern in both series is a projected charge-den-

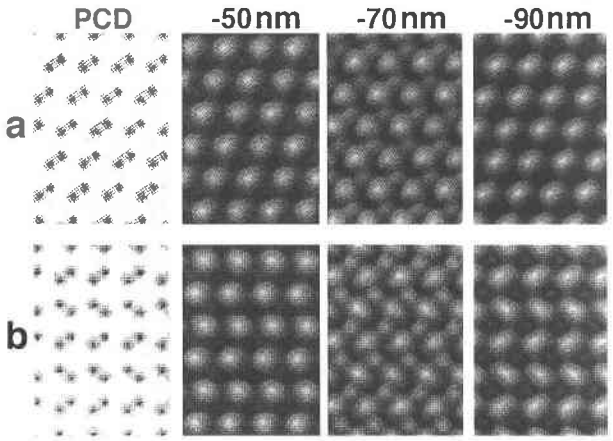

FIGURE 3. Projected charge-density (PCD) patterns and through-focus series of simulated electron micrographs of (**a**) ordered luzonite and (**b**) ordered enargite; the projections are the same as in Figure 1. The images were calculated for 200 kV and a crystal thickness of 6.8 nm. The objective defocus values are indicated for each image.

sity (PCD) map. The PCD patterns are directly related to the structures as seen in Figure 1; the double black spots correspond to pairs of metal and S atoms.

In the simulated electron micrographs, black contrast appears above the atom pairs at −50 nm defocus, but at −90 nm the black-spot contrast appears above the "tunnels" in the structures. The black and white spots are asymmetric over a range of defocus values, especially at −70 nm. From the positions and shapes of these "asymmetric dumbbells" it is possible to identify the positions of metal and S atoms within atom-pairs (Glaisher et al. 1989b; Smith et al. 1989).

Images were calculated for several types of faults in luzonite and enargite, including four faulted luzonite models (Fig. 4). The stacking sequences across the faults are represented within the boxed areas in the PCD patterns.

Using the ABC notation as defined in the introduction, the stacking sequence across a single stacking fault (↓) in luzonite is given as AbBcCaAbB↓aAbBcCa . . . (from bottom to top within the boxed area in Fig. 4a). Rotation twins are related by a 180° rotation around [221], the zone-axis that is perpendicular to the close-packed layers (Fig. 4b). The twin boundary (↕) is characterized by the AbBcCaAb↕BaAcCbBa . . . sequence. The AbB↓aAb sequence at the stacking fault and the Ab↕Ba sequence at the twin boundary indicate that these fault types introduce a three- and a two-layer-thick hcp (enargite) lamella into the ccp (luzonite) matrix, respectively (if, to be consistent with the observable contrast effects in HRTEM images, we regard the "Ab" sequence as a "layer").

At stacking faults and rotation twin boundaries the bonding configurations are the same as in the perfect structure; the metal-filled S-tetrahedra share corners, and their apices point in the same direction on both sides of the faults. Therefore, such faults do not affect the polarity of the crystal.

In reflection twins (Fig. 4c), the composition planes are mirror planes between the twin members, denoted by **C**. The stacking sequence of AbBcCaAbBc**C**cBbAaCcBb Aa**C**aAbBcC . . . shows that adjacent twin interfaces have different structures; boundaries characterized by face-sharing and corner-sharing tetrahedra alternate (marked + and −, respectively, in Fig. 4c).

The crystal parts on the two sides of an inversion boundary (Fig. 4d) can be transformed into each other by an inversion about the S atoms that lie in the plane of the boundary. Adjacent boundaries are different; the stacking sequence can be given as AbBcCa**A** aBbCcAaBbCcAa**B**

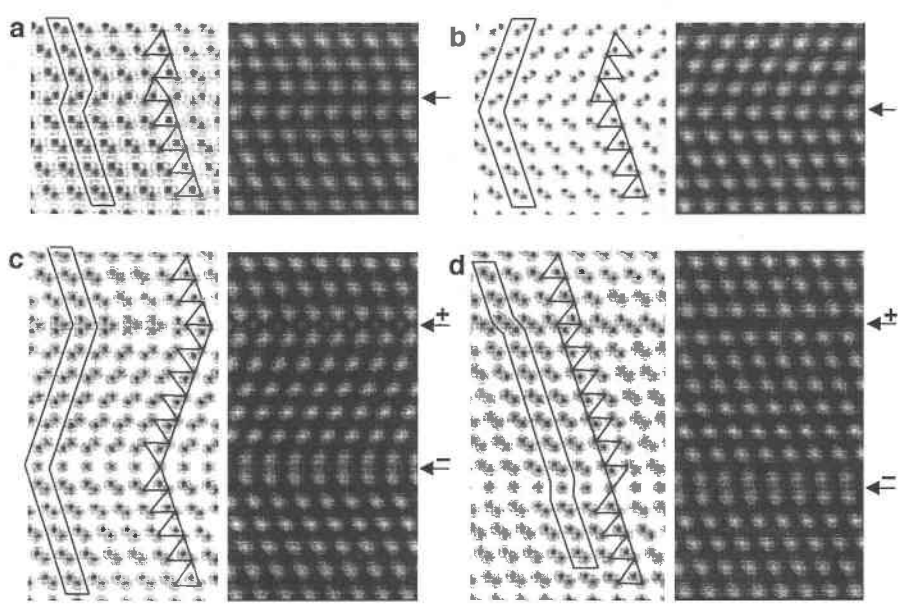

FIGURE 4. PCD patterns and simulated images for faulted luzonite structures. (**a**) Stacking fault; (**b**) Rotation twin boundary; (**c**) Reflection twin boundaries; (**d**) Inversion boundaries. The arrows mark the traces of the planes of the faults, and the tetrahedral coordinations of metal atoms are indicated by triangles. Stacking sequences for the boxed areas are given in the text. (200 kV accelerating voltage, 6.8 nm crystal thickness, and −50 nm defocus were used to calculate the HRTEM images.)

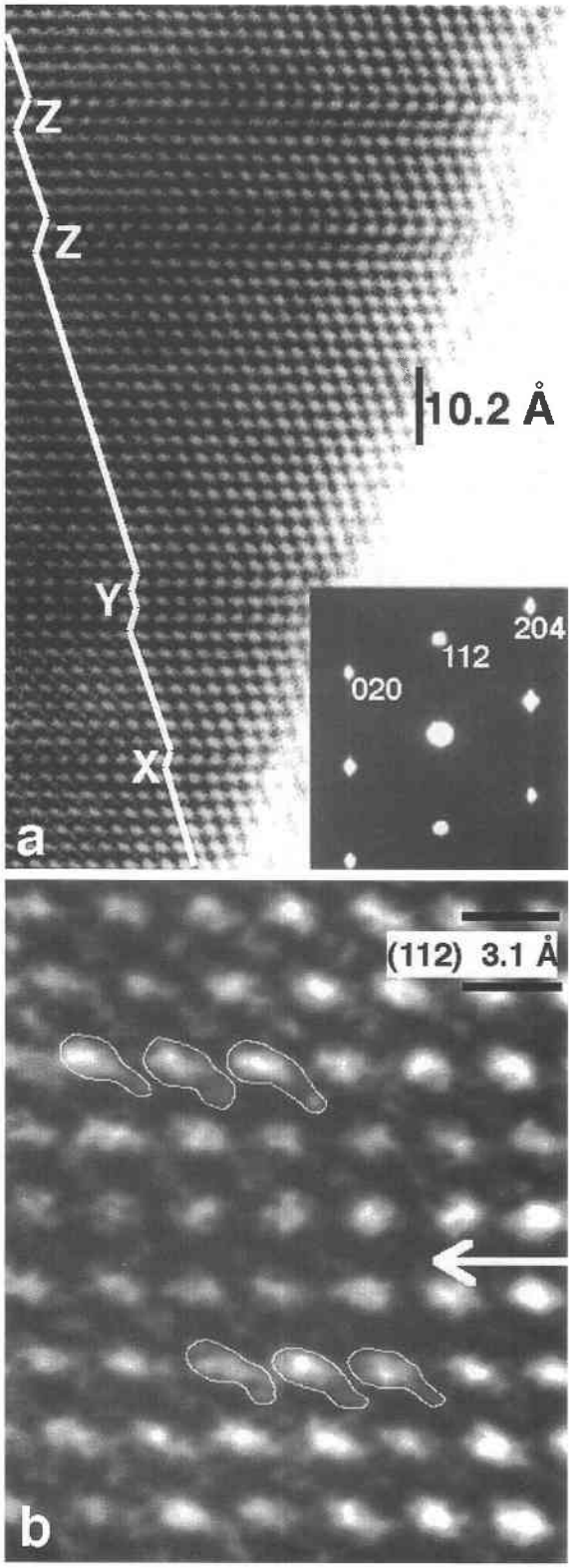

FIGURE 5. (**a**) [20$\bar{1}$] electron micrograph of a faulted luzonite crystal. At X, Y, and Z the regular ccp stacking is broken. (**b**) Enlarged image of the X fault in (**a**). The white arrow marks the plane of the fault.

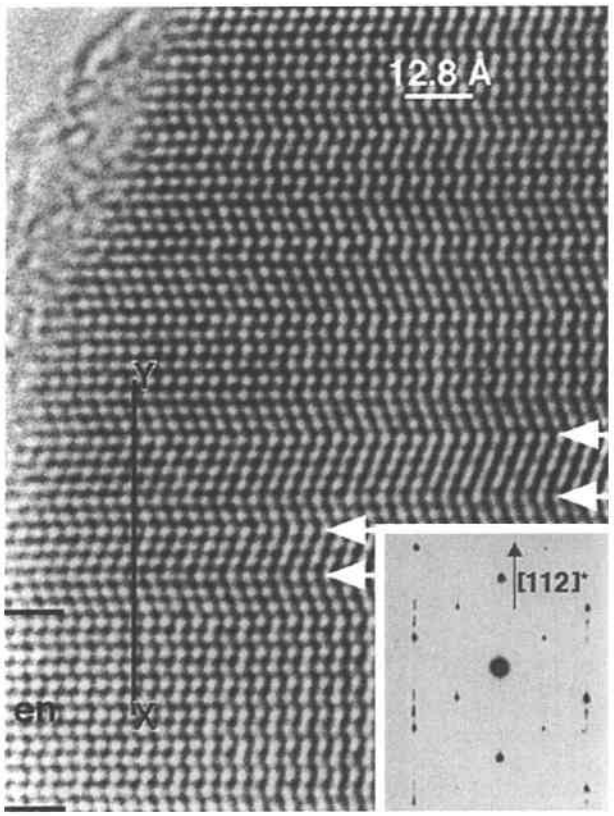

FIGURE 6. [1$\bar{1}$0] HRTEM image and SAED pattern of a heavily disordered luzonite fragment. Arrows and X, Y are discussed in text.

cCaAb . . . . At – boundaries the tetrahedra share corners and at + boundaries they share edges. The oppositely oriented metal-filled tetrahedra on the two sides of reflection twin boundaries and inversion faults indicate that the sense of the polar axis is opposite across these defects.

In the simulated electron micrographs of Figure 4, the different defect types produce distinct contrast effects; thus, the fault contrast can be used as a basis for the identification of fault types. However, our image simulations show that at certain values of crystal thickness and objective defocus (other than the ones used to produce the images in Fig. 4) it is difficult to distinguish stacking faults from inversion boundaries and rotation twins from reflection twins. In such cases an analysis of the asymmetric "dumbbell" contrast of black and white spots is useful. The shapes of the spots depend on the order of metal and S atoms within atom-pairs; therefore, we can determine whether the order of metal and S (i.e., the direction of polarity) is reversed across the boundary. If the polarities of different crystal parts are known, the atomic structure of the fault can be deduced.

Stacking disorder in luzonite

Luzonite crystals typically contain individual planar defects along the (112) planes. By analyzing the fault

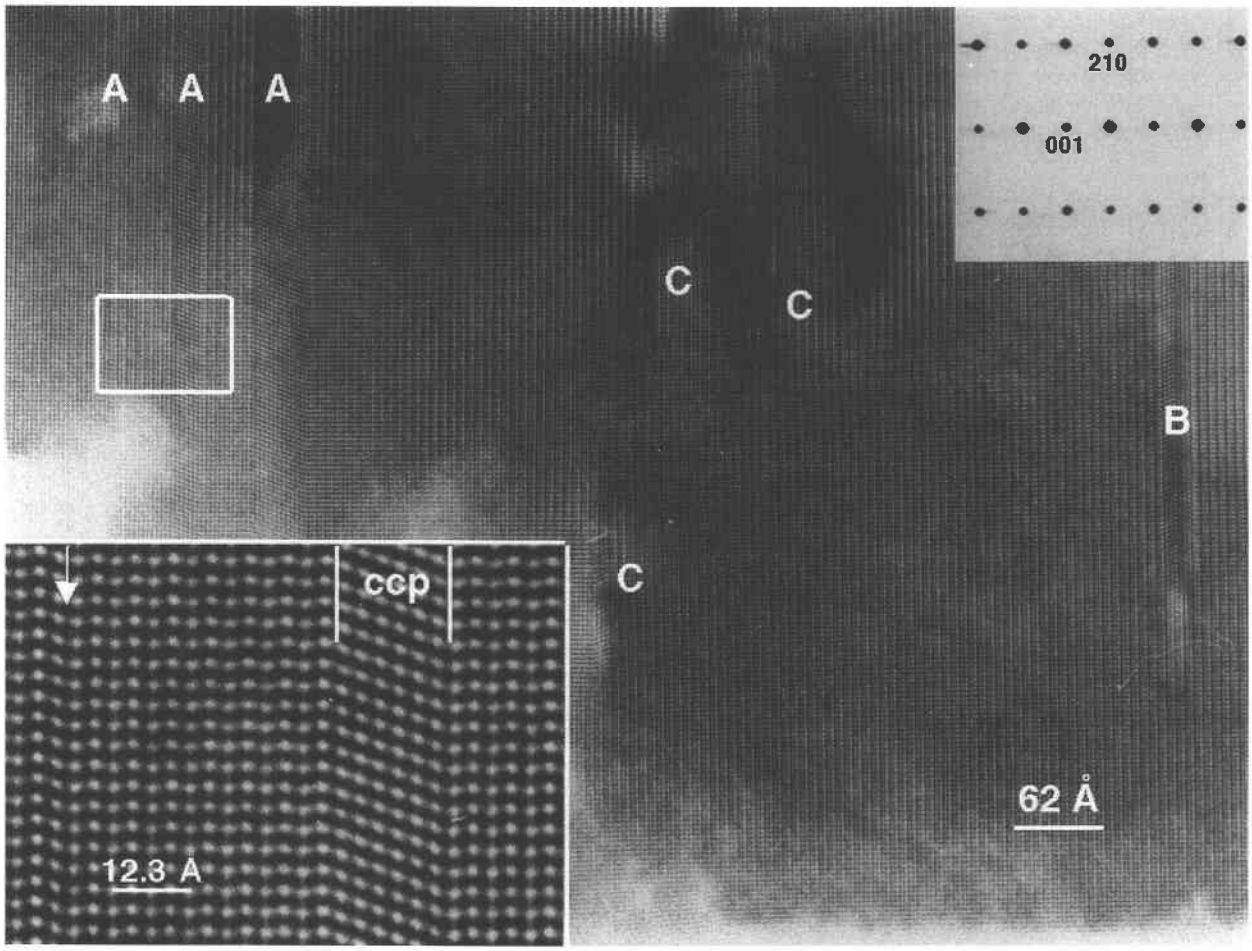

FIGURE 7. Low-magnification image of an enargite crystal containing several defects (marked A, B, and C). The boxed area is shown at high magnification by the inset in the lower left corner.

contrasts in Figure 5a, we find that all faults can be interpreted as stacking faults or rotation twin boundaries; hence, the polarity is the same over the whole crystal. The fault marked X is a simple stacking fault; its enlarged image is shown in Figure 5b. The white spots have asymmetric shapes on both sides of the fault, and they are elongated in the same direction (the right sides pointing down) both below and above the fault, indicating that the polarity is not reversed across the planar defect.

If stacking faults occur at every second close-packed layer, the product structure will have the ordered hexagonal sequence of enargite. A five-layer slab of the enargite structure appears at Y in Figure 5a. The two faults marked Z are identified as three-layer-thick rotation twins.

Some luzonite crystals exhibit heavily disordered structures. In addition to the reflections of luzonite, diffuse diffraction maxima appear in the SAED pattern of Figure 6. The additional spots result from twinning and the presence of units having hexagonal stacking sequences. The disordered stacking of white spots in the HRTEM image is best seen if the micrograph is viewed at a grazing angle along the XY line. The atom-pair positions can be mapped layer-by-layer from the image; if the symbols for metal atoms are omitted for simplicity, the stacking sequence from X to Y can be given as ABABABABCACBABCBACBCABA. This part of the crystal contains several rotation twin boundaries (marked by arrows) and a several-layer-thick slab with the ordered ABAB . . . sequence of the enargite structure (marked en).

Stacking disorder in enargite

Both faultless and disordered enargite crystals occur in the sample. Acicular crystal fragments seem to contain fewer faults than larger, plate-like fragments. Typically, the stacking defects (marked A in Fig. 7) run from edge to edge through the whole crystal. However, in some places terminating faults (B) and dislocation loops (C) also occur. The widths of the defects are variable; in the inserted magnified image the arrow marks a single stacking fault and "ccp" marks a seven-layer lamella with cubic stacking. The analysis of defect contrast reveals that in this crystal there are no polarity inversions at the single stacking faults or at the bands with cubic layer sequences.

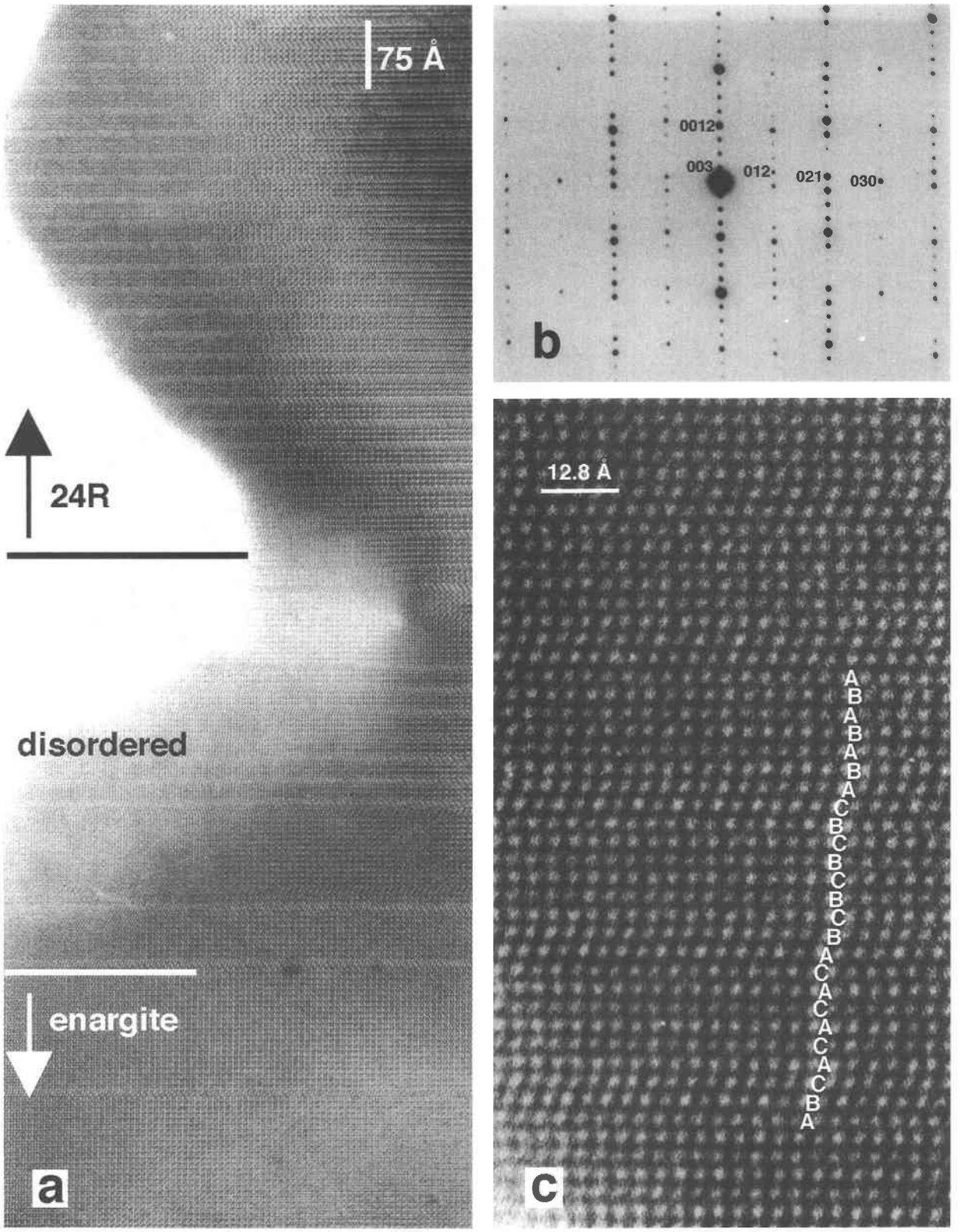

FIGURE 8. (a) Intergrowth between enargite and a 24R polytype. (b) [100] SAED pattern and (c) HRTEM image obtained from the 24R structure.

Polytypism in enargite

Two long-period, rhombohedral polytypes occur in the Recsk sample; both are intergrown with enargite. In the low-magnification micrograph (Fig. 8a) there is a disordered zone between enargite and an ordered superstructure. The superstructure extends over the rest of the ~0.5 μm long crystal. The systematic extinctions in the SAED pattern (Fig. 8b) reveal that the superstructure has a rhombohedral lattice; the only limiting condition for the appearance of reflections is $k + l = 3n$. The SAED pattern can be indexed on a hexagonal cell with $a = a_{enargite} = 0.741$, $c = 12c_{enargite} = 7.39$ nm. The HRTEM image (Fig. 8c) confirms that the structure consists of an ordered mixture of cubic and hexagonal layer sequences. The stacking sequence within one unit cell is given as ABCACACACABCBCBCBCABABAB. . . . Using more compact layer-stacking symbolism, the polytype can be described as 24R (Ramsdell notation) with $(311111)_3$ stacking (Zhdanov notation) (for a description of polytype notations, see Baronnet 1992).

Another rhombohedral, quasi-periodic polytype structure is shown in Figure 9. The two images were obtained from the same fragment, but at different defocus settings. The stacking sequence of atomic layers can be identified from Fig. 9a, whereas the changes of periodicity are easier to see in Fig. 9b. The black arrow marks a coherent boundary between ordered enargite and a 9R polytype. The stacking sequence of 9R is ABCBCACAB. . . , or $(21)_3$, as seen along the broken white line from A to B. The 9R stacking is interrupted by four-layered cubic sequences at several places (marked by white arrows).

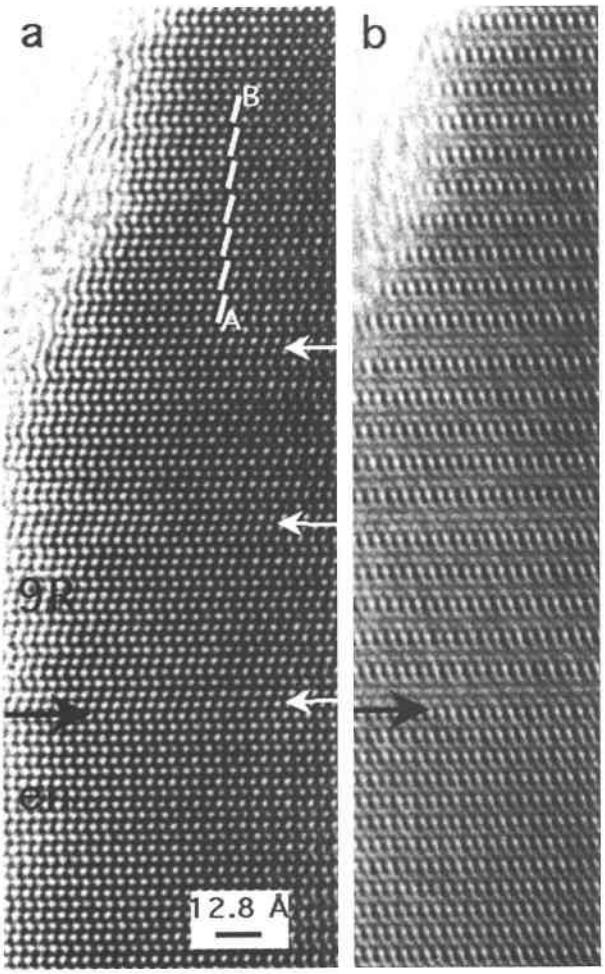

FIGURE 9. Intergrowth between enargite and a 9R polytype. The (**a**) and (**b**) images were taken at different defocus values. The black arrows mark the boundary between enargite and 9R, the white arrows indicate faults in the 9R sequence.

DISCUSSION

HRTEM images demonstrate the presence of common stacking faults and rotation twin boundaries in luzonite and the occurrence of stacking faults in enargite. We did not detect faults that would cause polarity inversions in these minerals.

Long-period, rhombohedral polytypes are unknown so far in $Cu_3(As,Sb)S_4$ minerals. However, several rhombohedral structures have been reported in structurally related materials. The 9R, $(21)_3$ structure was observed in GaSe by Terhell et al. (1975), and the 24R, $(311111)_3$ ZnS polytype was reported by Kiflawi et al. (1976), who observed that long-period polytypes formed spontaneously from vapor-grown crystals by solid-state transformation at room temperature.

The formation of the $(311111)_3$ stacking sequence can be explained using the periodic slip mechanism proposed by Mardix et al. (1968). If a crystal slip occurs periodically in a 2H structure, the resulting structure is a long-period polytype. The periodicity of the slips is ensured by a screw dislocation along **c**. The 24R, $(311111)_3$ structure forms if stacking faults occur every eight layers in enargite:

ABABABABABABABABABABABAB

AB↓CACACACACACACACACACA

ABCACACACA↓BCBCBCBCBCBCBC

ABCACACACACABCBCBC↓ABABAB

where the vertical arrow indicates the slip location. The periodic slip mechanism can also produce the 9R polytype but only from the 3C structure. However, such a conversion is unlikely, because both polytypes are intergrown with 2H enargite.

Owing to the stacking irregularities in their structures, luzonite and enargite are intergrown at the atomic level. Because a stacking fault produces a ccp lamella in the hcp matrix (and vice versa), a crystal with a disordered stacking sequence represents a transitional structural state between enargite (hcp) and luzonite (ccp).

The similarities of defect structures in ZnS to those in enargite and luzonite, suggest that studies of stacking

faults in ZnS could be relevant to Cu_3AsS_4 minerals as well. Several examples show that natural ZnS samples can be characterized by certain values of stacking fault densities and distributions. The structure of Pribram wurtzite consists of heavily disordered 2H and 3C sequences (Akizuki 1981); on the other hand, sphalerite polysynthetic twins are characteristic of the ZnS samples from Thomaston Dam (Fleet 1977) and Hosokura Mine (Akizuki 1981). Two types of disordered ZnS occur in Gyöngyösoroszi: "pyramidal" samples consist of densely twinned sphalerite, whereas in "radial" samples the structural disorder is similar to that of the Pribram wurtzite (Pósfai et al. 1988). Regardless of what mechanism formed these disordered ZnS structures (Akizuki 1983; Fleet 1983), their structural states can be modeled as if they would represent certain stages along the $2H \rightarrow 3C$ transformation.

The enargite-luzonite samples from Recsk cannot be characterized by uniform values of defect densities and distributions. Both ordered enargite and luzonite occur in the same specimens and apparently indicate the primary origin of these crystals. Enargite is the high-temperature modification of Cu_3AsS_4 (Skinner 1960; Lévy 1967); it is unlikely that it converted from luzonite by a solid-state transformation because the crystal habits typically correspond to those of orthorhombic enargite. For luzonite, solid-state transformation from enargite cannot be ruled out; however, on the basis of ore textures, we believe that luzonite is also a primary hydrothermal product. Therefore it seems that fluctuating conditions determined whether luzonite or enargite crystallized. The relationships between Sb-content and microstructure and the possible effects of temperature changes are discussed in a companion paper (Pósfai and Buseck 1998).

Acknowledgments

Transmission electron microscopy was performed at Stockholm University and made possible by a Swedish Institute scholarship to M. Pósfai. We thank István Dódony for discussions on defect types and Peter Buseck for a critical reading of the manuscript. The constructive reviews by Alain Baronnet and Peter Heaney are gratefully acknowledged.

References cited

Adiwidjaja, G. and Löhn, J. (1970) Strukturverfeinerung von Enargit, Cu_3AsS_4. Acta Crystallographica, B26, 1878–1879.

Akizuki, M. (1981) Investigation of phase transition of natural ZnS minerals by high resolution electron microscopy. American Mineralogist, 66, 1006–1012.

———(1983) Investigation of phase transition of natural ZnS minerals by high resolution electron microscopy: Reply. American Mineralogist, 68, 847–848.

Aminoff, G. and Broomé, B. (1931) Strukturtheoretische Studien über Zwillinge. I. Zeitschrift für Kristallographie, 80, 355–376.

Austerman, S.B. and Gehman, W.G. (1966) The inversion twin: prototype in beryllium oxide. Journal of Materials Science, 1, 249–260.

Baronnet, A. (1992) Polytypism and stacking disorder. In Mineralogical Society of America Reviews in Mineralogy, 27, 231–288.

Fleet, M.E. (1977) Structural transitions in natural ZnS. American Mineralogist, 62, 540–546.

———(1983) Investigation of phase transition of natural ZnS minerals by high resolution electron microscopy: discussion. American Mineralogist, 68, 845–846.

Gaines, R.V. (1957) Luzonite, famatinite and some related minerals. American Mineralogist, 42, 766–779.

Glaisher, R.W., Spargo, A.E.C., and Smith, D.J. (1989a) A theoretical analysis of HREM imaging for <110> tetrahedral semiconductors. Ultramicroscopy, 27, 19–34.

———(1989b) A systematic analysis of HREM imaging of wurtzite semiconductors. Ultramicroscopy, 27, 117–130.

———(1989c) A systematic analysis of HREM imaging of sphalerite semiconductors. Ultramicroscopy, 27, 131–150.

Kanazawa, Y. (1984) Synthesis and lattice constants of luzonite-famatinite crystals. Bulletin of the Geological Survey of Japan, 35, 13–17.

Kiely, C.J., Pond, R.C., Kenshole, G., and Rockett, A. (1991) A TEM study of the crystallography and defect structures of single crystal and polycrystalline copper indium diselenide. Philosophical Magazine, A63, 1249–1275.

Kiflawi, I., Kalman, Z.H., and Sonnenblick, Y. (1976) Direct observation of polytype transformations in a vapour-phase grown ZnS crystal. Journal of Crystal Growth, 34, 145–148.

Lévy, C. (1967) Contribution à la minéralogie des sulfures de cuivre du type Cu_xXS_4, 178 p. B.R.G.M., Paris.

Mardix, S., Kalman, Z.H., and Steinberger, I.T. (1968) Periodic slip processes and the formation of polytypes in zinc sulfide crystals. Acta Crystallographica, A24, 464–469.

Marumo, F. and Nowacki, W. (1967) A refinement of the crystal structure of luzonite, Cu_3AsS_4. Zeitschrift für Kristallographie, 124, 1–8.

Mizera, E., Sundberg, M., and Werner, P. (1984) Defect structure of ZnSe crystals investigated by electron microscopy. Physica Status Solidi, (a) 85, 83–88.

Morvai, G. (1982) Hungary. In F.W. Dunning, W. Mykura, and D. Slater, Eds., Mineral Deposits of Europe: 2. Southeast Europe, p. 13–54. The Mineralogical Society, London.

O'Keefe, M.A., Buseck, P.R., and Iijima, S. (1978) Computed crystal structure images for high-resolution electron microscopy. Nature, 274, 322–324.

Pósfai, M. (1991) Stacking disorder and cation ordering in some sulfide minerals with close-packed structures, Ph.D. thesis, Eötvös Loránd University, Budapest.

Pósfai, M. and Buseck, P.R. (1998) Relationships between microstructure and composition in enargite and luzonite. American Mineralogist, 83, 373–382.

Pósfai, M., Dódony, I., and Soós, M. (1988) Stacking disorder in the ZnS from Gyöngyösoroszi, Hungary. Neues Jahrbuch für Mineralogie Monatshefte, 10, 438–445.

Qin, L.C., Li, D.X., and Kuo, K.H. (1986) An HREM study of the defects in ZnS. Philosophical Magazine, A53, 543–555.

Shiojiri, M., Kaito, C., Sekimoto, S., and Nakamura, N. (1982) Polarity and inversion twins in ZnSe crystals observed by high-resolution electron microscopy. Philosophical Magazine, A46, 495–505.

Skinner, B.J. (1960) Assemblage enargite-famatinite, a possible geothermometer. Geological Society of America Bulletin, 71, 1975.

Smith, D.J., Glaisher, R.W., and Lu, P. (1989) Surface polarity determination in <110>-orientated compound semiconductors by high-resolution electron microscopy. Philosophical Magazine Letters, 59, 69–75.

Springer, G. (1969) Compositional variations in enargite and luzonite. Mineralium Deposita, 4, 72–74.

Sugaki, A., Kitakaze, A., and Shimizu, Y. (1982) Phase relations in the Cu_3AsS_4-Cu_3SbS_4 join. Science Reports of the Tohoku University, 3rd Series, XV, 257–271.

Sztrókay, K. (1944) Erzmikroskopische Beobachtungen an Erzen von Recsk in Ungarn. Neues Jahrbuch für Mineralogie, A79, 104–128.

Terhell, J.C.J.M., Lieth, R.M.A., and van der Vleuten, W.C. (1975) New polytypes in vapour grown GaSe. Materials Research Bulletin, 10, 577–582.

Manuscript received February 26, 1997
Manuscript accepted November 9, 1997